ISSN 1590-8844
International Journal of Mechanics and Control, Vol. 26, No. 01, 2025
https://doi.org/10.69076/jomac.2025.0002

PERFORMANCE AND EFFICIENCY PF A HYBRID SELF-PROPELLED CABLE LOGGING CARRIAGE: AN EXPERIMENTAL STUDY

Stefan Leitner[*,**] Lorenzo Maccioni[*] Giovanni Carabin [*] Raffaele Spinelli [***] Renato Vidoni[*,****]

[*] Free University of Bozen-Bolzano, Bolzano (Italy)
[**] LeitAlpin GmbH, Bolzano (Italy) - https://www.leitalpin.com/en
[***] Consiglio Nazionale delle Ricerche, Istituto per la Bioeconomia (CNR IBE), Sesto Fiorentino (Italy)
[****] Polytechnic Department of Engineering and Architecture, University of Udine, Udine (Italy)

ABSTRACT

Global warming and the dependance on expensive fossil fuels in uncertain times are two main drivers for the development of alternative drivetrains. The alpine logging sector is no exception. Indeed, electrification has demonstrated significant potential for fuel savings in cable logging applications, particularly due to the high capacity for energy recovery in cyclic operations involving variations in potential energy. This work presents results of a study involving several key sub-systems as well as the roundtrip efficiency of a hybrid self-propelled carriage called HULK. In addition to performance and efficiency studies of the engine-generator unit, energy dissipation unit and battery system, its two main drive systems, i.e., the dropline winch and the propulsion module, have been evaluated. The tests enabled the performance mapping of key components, identification of optimal operating points, and confirmation of the substantial energy recovery potential. Furthermore, the results highlight the feasibility of energy-autarkic operation in real-world transport applications.

Keywords: Drivetrain electrification, mechatronics, modelling, energy recovery, smart forestry

1 INTRODUCTION

Mechanization and automation are key to competing in today's fast-moving industries that demand ever higher productivity, product quality, traceability, reduced or safer personnel involvement and environmentally friendly operation. Moreover, to realize more environmentally-friendly vehicles and machines, promising solutions involve improving efficiency as well as energy recovery and regeneration, e.g. [1, 2, 3, 4]. This is also the case in the logging industry, especially in locations unsuitable for ground-based machinery operation where, thanks to the availability of new mechatronic and IoT technologies, smart and precision forestry concepts are gaining attention.

Cable logging solutions have a long history as the solution of choice to extract timber from difficult terrain, inaccessible to ground based vehicles. First cable logging solutions, primitive steam-powered apparatus, date back over 150 years [5]. Since then, yarders and carriages have undergone dramatic changes in multiple waves of innovation. Internal combustion engines, stepless hydraulic transmissions, and electronic control represent the most obvious major breakthroughs [6, 7]. The latest wave of innovation started around 10 years ago, with the introduction of the first electrified cable logging solutions [8, 9, 10]. The transition started with slack-pulling carriages, followed by tower yarders, dropline carriages and now also Self-Propelled Carriages (SPCs). A major challenge to overcome in the design of electrified cable logging equipment is to ensure reliable energy supply, given the inability to connect

Contact authors: S. Leitner[*], G. Carabin[*], Renato Vidoni[**],
[*] FiRST Lab, Free University of Bozen-Bolzano, 39100, Bolzano (I)
[**] Polytechnic Department of Engineering and Architecture, University of Udine, Via delle Scienze, 33100, Udine (I)
E-mail: stefan.leitner@unibz.it , giovanni.carabin@unibz.it , renato.vidoni@uniud.it

the equipment to the power grid. The first electric semi-automated carriages were presented in 2015 [11]. A more recent development is presented by the hybrid tower yarder K507e-H by Koller, i.e. series hybrid drivetrain, that stores recovered energy in an on-board high-voltage super-capacitor to be employed for the subsequent duty cycle [14]. Regenerative energy is complemented by an on-board engine-generator unit in start-stop control. Fuel savings have been shown to be almost 60 % compared to a conventional Diesel-hydraulic yarder in common cable yarding uphill setups. Fully electric models could be envisioned with large battery packs, to be charged by an external energy source when not in operation [15]. Energy supply to carriages offers more options. In the literature, a total of six energy supply concepts have been proposed for slack-pulling carriages, dropline carriages and SPCs [16]. Slack-pulling and dropline carriages require relatively little energy per cycle. Carriage-internal storage systems can be charged during lateral yarding, when lowering the payload, and/or while traveling along the cableway. SPCs need to also power the energy-hungry propulsion during out- and in-hauling, therefore requiring more extensive means of energy supply.

The latest development in the European cable yarding equipment sector is related to SPCs, i.e. fully motorized remote-controlled carriages capable of powering the extraction process without any additional equipment, with the presentation of an advanced prototype of a hybrid SPC by Leitalpin (Leitalpin GmbH, Bozen, Italy) named HULK [12]. So far, few studies have been presented on electrified cable logging equipment, and the existing literature provides insufficient knowledge about the performance and efficiency of these systems both in their main-subsystems and in actual applications.

This paper, starting from the preliminary results presented in [13], aims to provide an in-depth understanding of the performance and potential of energy recovery by the novel hybrid SPC prototype HULK, which in turn provides a better understanding of the amount of energy to be supplied by external means, i.e., via fuel.

The work is organized as follows: Section 2 describes the hybrid SPC HULK and its main subsystems. After that, data acquisition as well as test and simulation setup for the experimental evaluation are reported in Section 3. Results are presented and discussed in Section 4 together with considerations on their meaning for actual transport applications. This work is then concluded with an outlook on ongoing and future studies on this subject (Section 5).

2 THE HYBRID SELF-PROPELLED CARRIAGE: HULK

The hybrid SPC HULK, depicted in Fig.s 1a, 1b, is the main subject studied in this work. Its key features and technical specifications are reported in Table I.

Table I - Key Features and Specifications of the SPC HULK

Dimensions LxWxH	2.4 x 0.75 x 1.5 m
Max Power	150 kW
Propulsion Speed	0.1 - 11 m/s
Propulsion Force	2 - 50 kN
Winch Speed	0.1 - 5 m/s
Winch Force	2 - 45 kN
Max Skyline Slope	$\pm$ 120 %
Hybrid Series Configuration	
Adaptive Energy Management	
Target Control (automated skyline support crossing)	
Long Range Remote Control	
Twin-Cable Configuration	

The drivetrain architecture is a series hybrid concept with independent drives for the dropline winch and for carriage propulsion, see Fig. 1. The Power Distribution Unit (PDU) is at the center of this setup and serves as the interconnection between all drivetrain parts. The Energy Source (ES), made up of a gasoline engine, mechanical transmission parts and a generator-inverter set, supplies energy to the carriage if the regenerative energy is not sufficient to cover the energy needs of the machine cycle. An Energy Storage System (ESS) with discharging/charging efficiency $\eta_{ESS_{C/DC}}$ is connected to the PDU and stabilizes the system voltage by providing and drawing energy at a rate of $P_{PDU_{ESS}}$ as needed. $P_{PDU_{ESS}}$ can be estimated as the sum of the power of all connected devices. ES power ($P_{PDU_{ES}}$) is determined by the fuel consumption rate (Q_{FUEL}) and overall ES efficiency (η_{ES}). Since handling heavy loads from a higher to a lower elevation can lead to overcome the limit of recoverable energy, an Energy Dissipation (ED) system, realized in the form of a high performance fan and depicted in Fig. 1c, is installed to generate energy dissipation power ($P_{PDU_{ED}}$).

The power drawn from or supplied to the PDU by the drives ($P_{PDU_{DR}}$), i.e. winch and propulsion modules, is a function of: instantaneous drive force (F_{DR}) and speed (v_{DR}); and total drive module efficiency in motoring (η_{MOT}) or regeneration (η_{GEN}) mode. Motoring mode is typically associated with lifting a load and moving the carriage uphill, while regenerative mode corresponds to lowering a load and traversing versus the lower end of the cableway. Performance and efficiency studies are to be performed both on single modules, i.e. ES, ED and ESS units, as well as on roundtrip tests for both the winch ($\eta_{W_{RT}}$) and propulsion modules ($\eta_{P_{RT}}$).

For the former, i.e. single modules, both the ES and ED are independent systems, which can be tested at machine standstill. During regular operation of the SPC, generator torque is controlled based on the engine's load factor to optimize its efficiency at every operating point. The engine, in turn, is speed controlled based on a power set-point

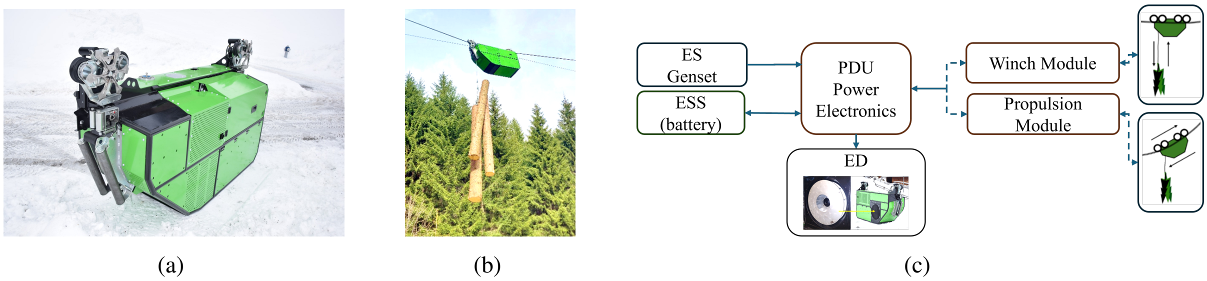

Figure 1 The HULK SPC: (a) and (b) the SPC advanced prototype; (c) Hulk main building blocks

computed within the energy management logic. For the ED, the fan is spun by a high-performance electric drive in power control, with cascading underlying torque and current control loops, respectively. The ED is activated by the SPC energy management logic to dissipate energy directly as it is generated at the drives, ensuring it occurs only during operation. The ESS employed in the SPCe is a power-density high-performance pack in the 800 V voltage range. Its power performance and efficiency are mainly determined by its impedance, which is highly dependent on the pack temperature and State-Of-Charge (SOC).

For the latter, i.e., roundtrip tests, the roundtrip efficiency analyzed in this study is defined as the percentage of energy recharged into the battery system during regeneration phases relative to the energy drawn from the battery during motoring phases. This is evaluated under the condition that the same mechanical work is performed on the carriage and/or payload during both motoring and regeneration phases.

3 EXPERIMENTAL SET-UP AND ROUNDTRIP TESTS SCENARIO

3.1 *Efficiency tests for ES, ED and ESS modules*

In this study, for the ES, the machine controller of the SPC was programmed in such a way that engine speed and generator torque could be controlled independently in predefined small steps. This allowed to set multiple speed-torque combinations.

For the ED, since the SPC offers an operational mode that allows direct control via the remote controller for testing and maintenance purposes, this mode was utilized to test the ED and gather performance data. Since the sole purpose of the ED is to remove excess energy from the system, its efficiency is mostly irrelevant. Still, it is desirable that the energy is dissipated directly at the fan, rather than converted to heat in the inverter-motor drive. In this study, the performance of the dissipation system drive components has been evaluated.

For the ESS, since pack impedance can only be determined indirectly by monitoring its voltage response to a change in current (or vice versa), to obtain responses at different cell temperatures and distinct SOC levels both for discharging and charging, an ad-hoc study has been performed: the pack was tested subjected to 10 kW of charging power (via the ES) and 25 kW of discharging power (via the ED) at various temperature-SOC operating points.

The data acquisition chain employed to obtain data during these tests is depicted in Fig. 2. CAN loggers, specifically of type CANedge1 of CSS Electronics were connected to the three CAN buses of the SPC to log and store the data. Every CANedge1 provides two independent channels, thus only two loggers were required. CAN bus data was stored in raw encrypted format on SD cards in the logging devices. The data were then converted and scaled to physical values via specifically developed Matlab code.

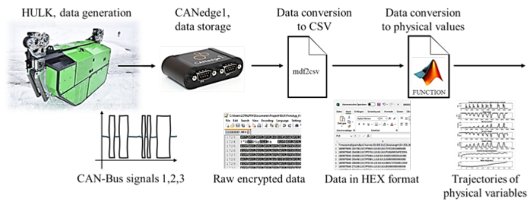

Figure 2 Data acquisition/conversion chain to obtain SPCe performance and efficiency data

3.2 *Roundtrip Efficiency Tests*

In 2024, a test campaign of the second prototype of HULK, an optimized version with respect to an earlier model tested after 2021, was performed by Leitalpin. Tests were carried out on a cableway installed by Leitalpin in the forests near Vipiteno, BZ, Italy. The installation concerned a standard standing skyline configuration, with a cableway length of about 400 m. The skyline had close to zero inclination at the lower end of the cableway, gradually rising to about 50 % slope versus the upper end of the installation. The objective of the tests were to obtain results of the roundtrip efficiencies of the winch and propulsion modules. Separate studies are carried out for the winch and the propulsion modules, evaluated via a combination of field tests and simulations.

Winch field tests consist of logging the winch motor torque during lifting ($T_{W_{LIFT}}(m_L)$) and lowering ($T_{W_{LOW}}(m_L)$) with various payloads, i.e, m_L between 0 kg and 2800 kg in steps of 700 kg.

Similarly, propulsion module field tests provide motor torque information for driving uphill ($T_{P_{UP}}$ (m_L,α_{SL})) and downhill ($T_{P_{DOWN}}$ (m_L,α_{SL})) for the same set of payloads, and for skyline inclinations α_{SL} in the range of 0 % to 50 %. Assuming constant efficiencies for the electric drives, consisting of the power electronics and the electric motors (η_{DR}) and the battery system (η_{BAT}), both during charging and discharging, drive torque in motoring and regeneration phases becomes proportional to the energy needed and recovered, respectively. In addition, since the roundtrip efficiency is a ratio-based measure, variables such as the distances covered or the drive speeds during the field studies are canceled out, simplifying the estimation of the roundtrip efficiencies in (1) for the winch and (2) for the propulsion module, respectively.

$$\eta_{W_{RT}} = \frac{T_{W_{LOW}}(m_L) \cdot (\eta_{DR} \cdot \eta_{BAT})^2}{T_{W_{LIFT}}(m_L)} \tag{1}$$

$$\eta_{P_{RT}} = \frac{T_{P_{DOWN}}(m_L, \alpha_{SL}) \cdot (\eta_{DR} \cdot \eta_{BAT})^2}{T_{P_{UP}}(m_L, \alpha_{SL})} \tag{2}$$

η_{DR} and η_{BAT} were estimated thanks to the results of the single modules efficiency tests reported in the next section.

4 RESULTS AND DISCUSSION

4.1 ES, ED, ESS Modules

4.1.1 ES: Energy Source

A total of 120 engine speed-generator-torque combinations has been tested and engine speed, engine fuel consumption and ES power data collected. By setting the genset electrical output power in relation to the input power equivalent of the fuel consumption rate, the total genset efficiency can be determined through Eq. (3):

$$\eta_{ES} = \frac{P_{PDU_{ES}}}{Q_{FUEL} \cdot \gamma_{FUEL}} \tag{3}$$

where γ_{FUEL} is the specific energy density of gasoline (approx. 34.2 MJ/l or 9.5 kWh/l [18]).
In Table II the estimated results η_{ES} across the operating points given by Eq. (2) are reported while in Fig. 3 a visual representation is given.
As can be appreciated, the η_{ES} generally increases with the generator torque. Moreover, around 1800 rpm (close to minimum/idling speed) and 3000 rpm (engine nominal speed), (local) efficiency maxima are computed. While the former results in the largest η_{ES} of about 33.9 % at 45 Nm torque, the latter appears to be an ideal trade-off for power and efficiency, with an η_{ES} of about 25.6 % at 45 Nm torque.

4.1.2 Energy Dissipation System

To test the ED system, nine power levels from 5 kW up to a maximum of 50 kW were evaluated. The data have been collected by manually controlling the dissipation system. At peak performance, the dissipation system could reach about 100 kW of power at a speed of 7000 rpm, with the tangential speed of the dissipation system reaching Mach 0.55. Fig. 4 reports the trends of seven key dissipation system performance variables that are:

1. Torque-limit and set-point: The torque limit in speed control and the torque set-point in torque control sent to the inverter, given in Nm;
2. Motor speed: The motor speed driving the fan, given in rpm. Based on an arbitrary convention by Leitalpin, the propeller rotates in the negative direction;
3. DC bus current: The current flowing into the inverter at the HV DC terminals. This corresponds to the battery discharge current if no other loads are active;
4. DC bus voltage: The voltage at the inverter HV input DC terminals. This voltage follows the battery terminal voltage very closely;
5. Output voltage: The output voltage corresponds to the RMS voltage of the three-phase sinusoidal inverter output (motor input) voltage;
6. Inverter hot spot temperature: The temperature measured at the highest temperature point within the inverter. It corresponds to a measure close to the power semiconductors;
7. Motor temperature: The temperature measured within the stator windings of the PMSM machine.

Table II - ES efficiency as a function of engine speed and generator torque

Engine Speed [rpm]	*Generator Torque [Nm]* 0	5.0	10.0	15.0	20.0	25.0	30.0	35.0	40.0	45.0
1750	0.0	5.5	12.9	17.5	25.3	24.0	29.7	27.1	28.2	27.6
1800	0.0	4.3	15.4	18.5	21.4	28.0	31.1	30.7	31.8	33.9
1900	0.0	13.8	15.0	15.3	25.1	25.8	28.9	29.2	30.2	30.5
2000	0.0	7.6	8.8	11.3	13.9	17.8	19.6	20.1	22.5	21.7
2200	0.0	4.5	8.4	10.7	16.7	15.3	15.8	18.5	18.2	19.3
2400	0.0	7.2	7.7	14.4	14.4	16.5	17.3	18.9	19.3	19.3
2600	0.0	6.4	14.7	18.9	17.1	20.0	18.9	21.8	21.6	19.6
2800	0.0	6.2	14.9	18.0	19.6	22.3	21.4	21.6	21.5	20.0
3000	0.0	7.1	14.4	18.1	20.6	25.9	24.4	24.9	25.2	25.6
3200	0.0	4.7	9.4	14.1	19.2	22.2	23.1	23.6	23.9	20.2
3400	0.0	2.8	6.6	9.7	11.6	16.4	15.0	17.8	18.4	18.1
3600	0.0	3.8	6.9	10.8	11.8	17.1	17.3	18.4	17.8	17.2

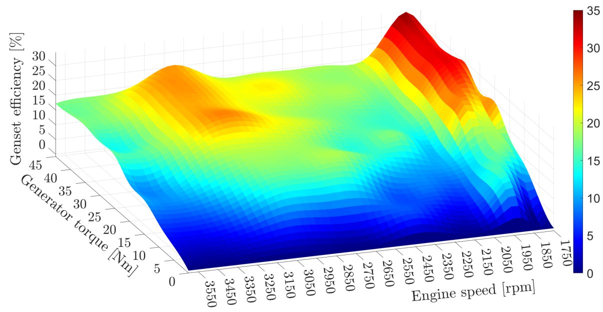

Figure 3 ES efficiency as a function of engine speed and generator torque: visual representation

ISSN 1590-8844
International Journal of Mechanics and Control, Vol. 26, No. 01, 2025

The shape of the curves during operation, controlled by the energy management logic, depends on many operation variables and, while transitory data may only serve as an example, steady state data represent commonly expected operating points.

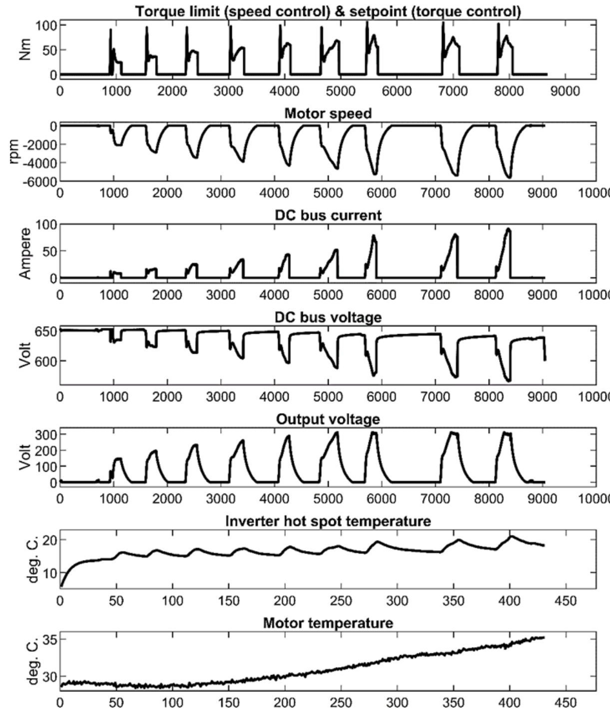

Figure 4 ED system: 7 key dissipation system performance variables during a test involving a tot. of 9 power levels (5 kW- 50 kW). X-axis: n° of samples during data acquisition

For each of the nine operating points, the product of the steady state values of DC bus current and voltage results in the electrical power input into the inverter. Similarly, the final steady state values of fan speed and torque define the mechanical output power of the motor. This provides nine independent propeller drive efficiency estimates at nine distinct operating points, as computed and reported in Table III. Through the inverter, current, voltage and speed are accurately measured. Motor torque is indirectly estimated by the inverter based on motor stator current measurements exploiting a simple linear model and the motor torque constant K_T [Nm/A]. Slight discrepancies between the K_T setting and actual motor properties, as well as nonlinear effects such as magnetic saturation can cause considerable deviations in the estimated vs. the generated torque. From the estimations, it clearly resulted that the K_T setting is too large since the inverter-motor efficiency will never reach 100 %. At the optimal operating point, the efficiency should reach about 95 %. A good approximation to the actual performance can thus be accomplished by down-scaling motor torque by a factor of 0.95 and re-estimating the motor output power and efficiency, accordingly. In Tab. III, data on which this compensation has been applied are labeled by (*). Looking at the electrical power draw from the dissipation system with respect to the motor speed, a non linear relationship (as foreseeable) can be appreciated, see Fig. 5. Indeed, while axial fans tend to have a somewhat torque-

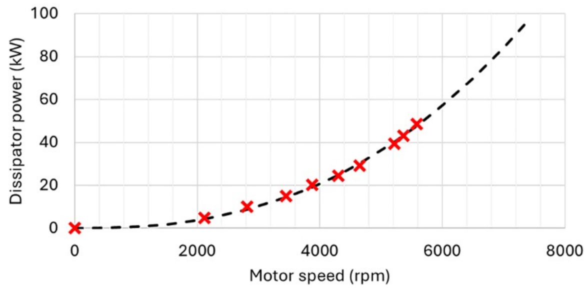

Figure 5 ED system: power drawn as a function of dissipation system motor speed n_{ED}

speed linear relationship, centrifugal fans typically follow a quadratic behavior. The dissipation system of the SPCe resembles a centrifugal fan but since there is limited space within the machine and the air flow is significantly restricted by the protective cover, torque does not rise in a quadratic way with speed but the dissipation system power $P_{PDU_{ED}}$ follows the following approximated behavior:

$$P_{PDU_{ED}} = k_{PDU_{UP}} \cdot n_{ED}^{2.5} \qquad (4)$$

where n_{ED} is the fan speed in (rpm), $k_{PDU_{UP}}$ the estimated coefficient = $2.05 \cdot 10^{-8}$ and $P_{PDU_{ED}}$ is the dissipation system power in (kW).
From the curves shown in Fig. 4, looking at inverter hot spot and motor temperatures, their overall temperature rise is very similar. This indicates that they match well from a thermal (performance) standpoint. The thermal time constant (and capacity) is larger in the motor with respect to the inverter, such that its temperature does not respond swiftly to load changes. The power semiconductor in the inverter cannot absorb a lot of thermal energy and thus responds swiftly to current changes.

4.1.3 ESS: Energy Storage System

Tests were performed to characterize the ESS at different temperatures and distinct SOC levels both for charging (10 kW) and discharging (25 kW). Tested cell temperature levels are 5.5 °C (corresponding to air temperature), 11.4 °C and 16.6 °C. % SOC levels of 32 %, 45 %, 58 % and 71 % were evaluated. In Tab. IV the pack voltage rise and drop test results are reported together with the Open Circuit Voltages (OCV) at each of the SOC levels. Negative results report the pack voltage drop (ΔV_{ESS}) in response to 25 kW of power (drawn by the dissipation system), whereas positive results indicate a pack voltage rise (ΔV_{ESS}) in response to

Table III - ED system: electrical and mechanical performance and efficiency (torque corrected by a factor of 0.95

Operating point	1	2	3	4	5	6	7	8	9
DC Bus Current [A]	7.8	16.1	24.3	33.3	41.1	49.2	67.3	75.2	85.1
DC Bus Voltage [V]	634.9	623.2	613.3	605.8	597.4	591.8	583.9	573.8	569.5
IN-Electric Power [kW]	5	10	14.9	20.2	24.6	29.1	39.3	43.2	48.5
Motor Speed [rpm]	2114	2812	3449	3877	4303	4654	5219	5363	5584
Motor Torque [Nm]	21	33	41	50	54	58	69	73	78
Motor Torque*[Nm]	20	31	39	47	51	55	65	69	74
OUT-Mech Power*[kW]	4.4	9.2	14.1	19.3	23.1	26.9	35.8	38.9	43.3
Efficiency [%]	88	92	94	95	94	92	91	90	89

10 kW charging power. After completing the tests at the first temperature level, the pack was heated up to the other temperatures of interest with the help of the onboard thermal management system. Voltage responses were obtained at four SOC levels, by discharging the pack consecutively to the previously established levels. The DC impedance Z_{ESS}

Table IV - ESS system: measured battery pack terminal voltage drop and rise [V] with respect to the battery SOC and average cell temperature

		Discharging (25 kW)				Charging (10 kW)			
	SOC [%]	32	45	58	71	32	45	58	71
	OCV [V]	626	668	702	732	626	668	702	732
	5.5	-52	-39	-33	-30	19	20	20	21
	11.4	-43	-32	-28	-25	15	15	16	17
	16.6	-34	-25	-20	-16	11	13	12	13
Av. cell. temp	22.3	-25	-18	-14	-12	8	9	9	10
(°C)	28.5	-20	-15	-12	-10	5	5	6	8

of the battery pack can be computed for each operating point through the Eq. (5):

$$Z_{ESS} = \frac{(OCV + \Delta V_{ESS}) \cdot \Delta V_{ESS}}{P_{PDU_{ESS}}} \tag{5}$$

and the pack efficiency can be obtained through the following:

$$\eta_{ESS_{C/DC}} = \frac{P_{PDU_{ESS}} - \dfrac{\Delta V_{ESS}^2}{Z_{ESS}}}{P_{PDU_{ESS}}} \tag{6}$$

In Fig. 6, Z_{ESS} is shown through 3D surface plots with respect to SOC and cell temperature levels for discharging (Fig. 6a) and charging (Fig. 6b). As could be expected, cell temperature has a large impact on Z_{ESS} both during charging and discharging: the estimated pack DC impedance is 2.5 to 4 times higher than at the maximum tested temperature. As a consequence, at low temperatures the battery responds to load changes with large voltage changes. Moreover, as it can be expected, the pack impedance increases with the discharging of the battery. Looking at the estimations with respect to the SOC, larger discharge power can be better handled by a well charged than by a near depletion battery. Estimations show that at 28.5 °C, the Z_{ESS} increases by

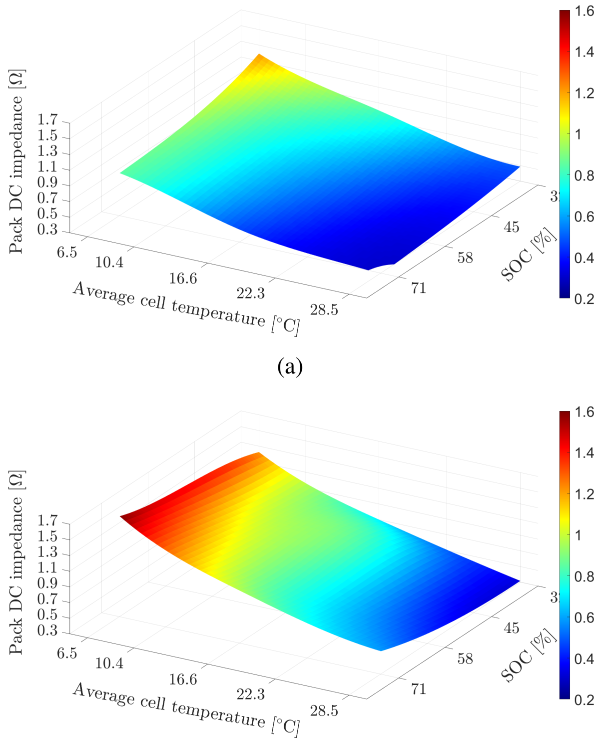

Figure 6 ESS: battery pack DC impedance in charging (a) and discharging (b) wrt SOC and average cell temperature

68 % when discharging between 71 % and 32 % SOC. The reverse is true when charging: indeed, still at 28.5 °C, Z_{ESS} shows the maximum increase of 88 % between 32 % and 71 % SOC. The minimum estimated Z_{ESS} value is 290 mΩ (discharging at 28.5 °C and 71 % SOC) while the maximum is 1.59 Ω (charging at 5.5 °C and 71 % SOC). From these data and charts, the target operating point for the battery pack within the SPC to perform a large number of high-power micro-cycles can be selected at 58 % SOC and 28.5 °C, that correspond also to 702 V OCV, 330 mΩ and 430 mΩ Z_{ESS} for discharging and charging, respectively.

Given the selected operating point, $\eta_{ESS_{C/DC}}$ can be evaluated through Eq. (6). For an ESS of -120 kW, $\eta_{ESS_{C/DC}}$ results in 90.3 % and increases through the lowering of the power (discharging) up to the theoretical value of 100 % at 0 kW. Then, while increasing the power from o to 120 kW (charging), $\eta_{ESS_{C/DC}}$ decreases up to 86.5 %. In general, increasing power (i.e. current), leads to an increase of losses.

4.2 Roundtrip Tests

4.2.1 Winch Module

As reported, winch field tests consisted of logging the winch motor torque during lifting and lowering with various payloads. In Fig. 7, the field measurements results are shown. The motor torque trends follow almost straight lines when plotted against varying payload mass, both when lowering and lifting the payload. They can be respectively

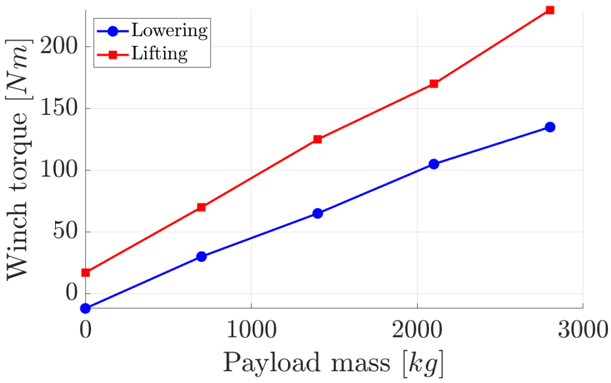

Figure 7 Winch motor torque during lifting and lowering as a function of the payload mass

approximated by Eq.s (7) and (8), where $T_{W_{LOW}}$ and $T_{W_{LIFT}}$ are expressed in Nm and m_L is expressed in kg:

$$T_{W_{LOW}}(m_L) = k_{W_{LOW}} \cdot m_L + T_{W_{LOW_0}} \tag{7}$$

$$T_{W_{LIFT}}(m_L) = k_{W_{LIFT}} \cdot m_L + T_{W_{LIFT_0}} \tag{8}$$

with $T_{W_{LOW_0}}$ = - 9.2 Nm, $k_{W_{LOW}}$ = 0.0527 m^2/s^2, $T_{W_{LIFT_0}}$ = 17.2 Nm and $k_{W_{LIFT}}$ = 0.0751 m^2/s^2. The maximum error between the measured and the estimated result is less than 4.9 Nm. Substituting Eq.s (7), and (8) into Eq. (1) yields an explicit solution of the approximate winch roundtrip efficiency of HULK as a function of payload mass. The estimations are plotted in Fig. 8. It shows that approximately 180 kg of payload is required to overcome mechanical losses in the system, enabling the winch drive to enter regeneration mode when lowering the payload. Up to this loading condition, the roundtrip efficiency is zero. The efficiency then continues to rise with an increasing payload, reaching 47.5 % at the maximum tested payload of 2800 kg. It

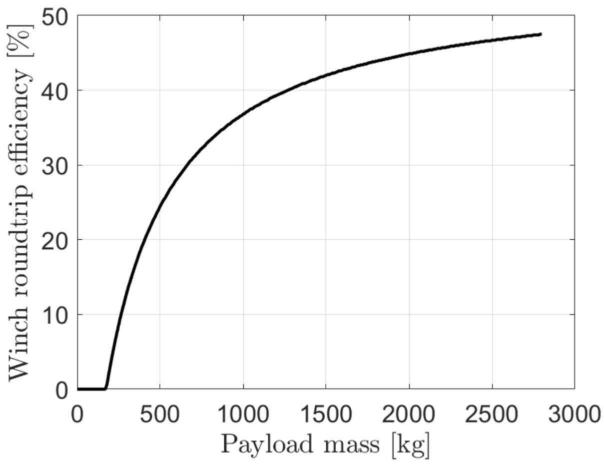

Figure 8 Roundtrip efficiency of the hybrid SPC when operating the winch, as a function of the payload mass

appears to asymptotically approach about 50 % at a very large payload. The winch roundtrip efficiency can also be interpreted as the ratio of lifting over lowering distance required to maintain a constant state of charge level of the battery system, i.e. at a payload of 800 kg, where the efficiency reaches 1/3 or 33 %, recovering the energy invested to lift the load by X meters requires it to be lowered by 3X meters.

4.2.2 Propulsion Module

Propulsion module field tests provide motor torque information for driving uphill and downhill for the same set of payloads previously reported, and for skyline inclinations in the range of 0 % to 50 %. Test results are reported in Fig. 9 and 10 Motor torque curves are provided for five different loading conditions, both when driving uphill and downhill. Given that the maximum skyline inclination at the test installation was 50 %, results have been extended to slopes of 100 % via mathematical extrapolation, depicted via dashed lines. The gradient and offset coefficients describing each of these extrapolations can in turn be approximated via linear expressions, yielding explicit solutions for the propulsion torque in uphill $T_{P_{UP}}$ (Nm) and downhill $T_{P_{DOWN}}$ (Nm) transport as a function of payload mass and skyline inclination α_{SL} (in %) respectively as given by Eq.s (9) and (10):

$$T_{P_{UP}}(m_L, \alpha_{SL}) = (k_{P_{UP_{0\%}}} \cdot m_L + T_{P_{UP_{0\%}}}) \cdot \alpha_{SL} + k_{P_{UP_0}} \cdot m_L + \\ + T_{P_{UP_0}} \tag{9}$$

where $T_{P_{UP_0}}$ = 37.857 Nm, $k_{P_{UP_0}}$ = 0.028 m^2/s^2, $T_{P_{UP_{0\%}}}$ = 1.774 Nm/% and $k_{P_{UP_{0\%}}}$ = 0.0009 m^2/s^2%;

$$T_{P_{DOWN}}(m_L, \alpha_{SL}) = (k_{P_{DOWN_{0\%}}} \cdot m_L + T_{P_{DOWN_{0\%}}}) \cdot \alpha_{SL} + \\ + k_{P_{DOWN_0}} \cdot m_L + T_{P_{DOWN_0}} \tag{10}$$

where $T_{P_{DOWN_0}}$ = 24.095 Nm, $k_{P_{DOWN_0}}$ = - 0.013 m^2/s^2, $T_{P_{DOWN_{0\%}}}$ = 0.583 Nm/% and $k_{P_{DOWN_{0\%}}}$ = 0.0016 m^2/s^2%.

ISSN 1590-8844
International Journal of Mechanics and Control, Vol. 26, No. 01, 2025

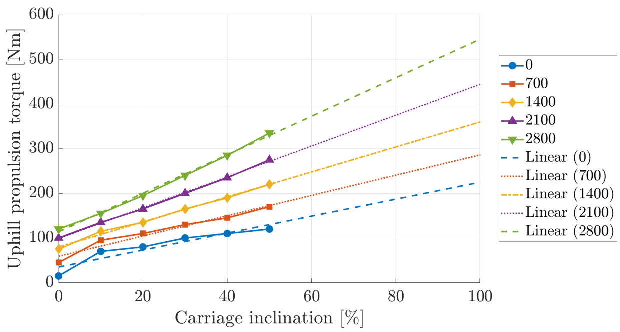

Figure 9 Propulsion motor torque when driving uphill, as a function of the payload mass and carriage inclination.

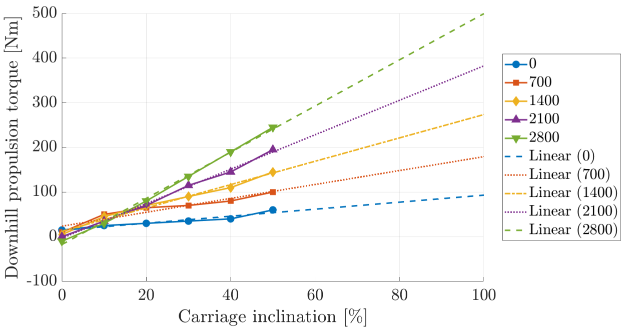

Figure 10 Propulsion motor torque when driving downhill, as a function of the payload mass and carriage inclination.

The average approximation error across the entire input range is 2.2 Nm for Eq. (9) and 0.6 Nm for Eq. (10). Substituting Eq.s (10) and (9) into Eq. (2) yields an explicit solution of the approximate propulsion module roundtrip efficiency of HULK as a function of payload mass and skyline inclination. The estimated results are presented in Fig. 11. With no skyline inclination ($\alpha_{SL} = 0\%$), the result of Eq. (2) can be negative, in which case it is kept at zero. With low payloads or small inclinations, there is only little potential for energy recovery. However, the weight of the carriage when moving uphill still draws significant power. Consequently, in these cases, the roundtrip efficiency is only as high as 1/3 or lower. As expected, the efficiency rises with increasing payload and slope, ultimately reaching a maximum of 70.6 % when both these variables are maximized. The operating condition where both the payload and the slope are simultaneously very small results in an anomaly in terms of the expected result. Fig. 11 indicates an efficiency rise to 49.7 % at the (0,0) point. This effect can be explained with the help of Fig. 12.

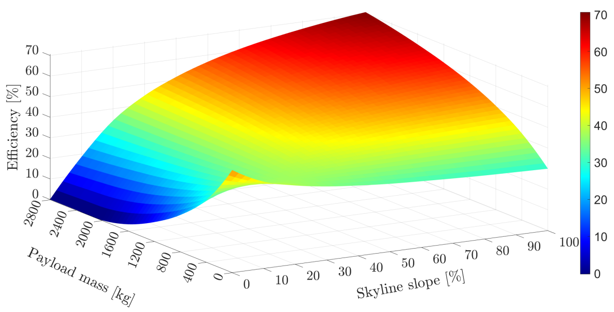

Figure 11 Roundtrip efficiency of the hybrid SPC when operating the propulsion module.

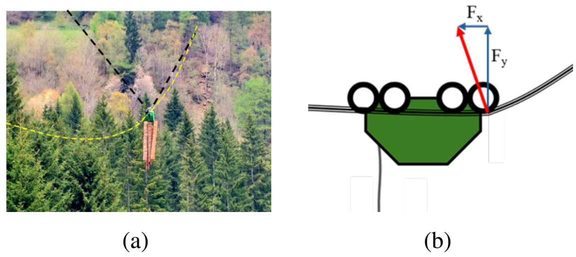

Figure 12 Impact of the skyline curvature on the propulsion force of HULK

The skyline slope in this work pertains to the slope of the skyline at the current carriage location, which is equivalent to the inclination of the carriage itself. As can be seen from the picture (Fig. 12a), the skyline (highlighted by the black dashed line) is significantly deflected by HULK. While the section of skyline behind HULK is close to horizontal, the section in front of it is rising at a considerable rate. As indicated by the sketch in Fig. 12b, this leads to a horizontal force component F_x, tending to force HULK in the downward direction, despite it resting on the (close to) horizontal skyline. Force F_x provides potential for energy recovery when moving downhill/backward on the flat skyline, consequently yielding increased efficiency. With rising payload, F_x becomes less relevant with respect to other forces, leading to a drop of the roundtrip efficiency.

Overall, results have shown substantial potential for energy recovery. However, unless the load is lowered much further at the landing site than it is yarded laterally and lifted in the felling area, the winch system cannot be self-sufficient. Its large gear reduction ratio leads to relatively low efficiency during the lowering phase, approaching 50 % at high loads. The reduction ratio in the propulsion module is significantly smaller, its maximum roundtrip efficiency therefore substantially higher. Moreover, in downhill transport, the carriage drives uphill unloaded. Results clearly show that the regeneration torque when moving downhill loaded can be much higher than the torque required to move uphill un-loaded. Computing the roundtrip efficiency with such different loading conditions would yield values significantly beyond 100 %. It is therefore reasonable to expect that the surplus of recovered energy from retarding the loaded carriage downhill can also compensate for the lack of energy to complete the winching cycle. Thus, energy autarkic operation appears possible.

5 CONCLUSIONS

Alpine logging operations can benefit from hybridization or electrification of the equipment. In the recent past, the first hybrid and fully electric solutions emerged. The aim of this paper was to study several key sub-systems as well as the roundtrip efficiency of a hybrid self-propelled carriage, i.e. one of the latest innovations of this industry. In particular, engine-generator set, energy dissipation unit and battery pack were firstly tested with the machine at standstill. Results show that the engine-generator set can achieve an overall efficiency of up to 33.9 %, the battery system can supply a power of 120 kW with less than 10 % of losses, the winch a maximum roundtrip efficiency of 47.5 %, while the propulsion module an efficiency of up to 70.6%. All these results confirm the large potential for energy recovery and the potential of energy-autarkic operation in real-world transport applications. Future work will focus on extended fuel consumption studies, as well as studies of the fuel saving potential with respect to conventional SPCs and tower yarders. Another area of interest is to draw out the boundaries of transport characteristics in downhill setups to ensure HULK can operate energy autarkic.

Acknowledgments

This study was carried out within the Agritech National Research Center (Task 4.1.4) and received funding from the European Union Next-GenerationEU (PIANO NAZIONALE DI RIPRESA E RESILIENZA (PNRR) – MISSIONE 4 COMPONENTE 2, INVESTIMENTO 1.4 – D.D. 1032 17/06/2022, CN00000022).

REFERENCES

[1] Sholanov K., Omarov A., Ceccarelli M., Improving efficiency of converting wind energy in modified sail wind power station, *Int. Journal of Mechanics and Control*, ISSN 1590-8844, 23, 02, pp. 101-110, 2022.

[2] Castellano A., Cammalleri M., Optimal operation of power-split hybrid electric powertrain: comparison between two performance indices, *Int. Journal of Mechanics and Control*, ISSN 1590-8844, 23, 01, pp. 3-14, 2022.

[3] Logozzo S., Valigi M.C., Green tribology: wear evaluation methods for sustainability purposes, *Int. Journal of Mechanics and Control*, ISSN 1590-8844, 23, 01, pp. 23-34, 2022.

[4] Scalera L., Carabin, G., Vidoni, R., Wongratanaphisan, T., Energy Efficiency in a 4-DOF Parallel Robot Featuring Compliant Elements, *Int. Journal of Mechanics and Control*, ISSN 1590-8844, 20, 02, pp. 49-57, 2019.

[5] Visser R., Harrill H., Cable yarding in North America and New Zealand: A review of developments and practices. *In Croatian Journal of Forest Engineering*, 38-2, pp. 209–217, 2017.

[6] Harrill H., Visser R., A review of cable logging literature. *Rotorua, New Zealand: Future Forests Research Ltd.*, Report No.: H019. 17, 2014.

[7] Heinimann H.R., Stampfer K., Loschek J., Caminada L., Perspectives on Central European Cable Yarding Systems. *Austrian Journal of Forest Science*, 123-3, pp. 121-139, 2006.

[8] Varch T., et al., Advances in Cable Yarding: A Review of Recent Developments in Skyline Carriage Technology. *Current Forestry Reports*, 7, pp. 181–194, 2021.

[9] Vorraber M., Produktivität bei der Holzrückung mit dem Mast-seilgerät Koller K 307C-H und dem energierückgewinnenden Laufwagen ESK 2.0. [Productivity of timber extraction with the tower yarder Koller K 307C-H and the energy-recuperating carriage ESK 2.0]. *MS Thesis*, Vienna (Austria): University of Natural Resources and Life Sciences Vienna, 47 p., 2020.

[10] Varch T., et al., Productivity, fuel consumption and cost in whole tree cable yarding: conventional diesel carriage versus electrical energy-recuperating carriage. *International Journal of Forest Engineering*, 32(sup1), 20–30, 2020.

[11] Raymond K., Visser R., Harvesting technology watch, Future Forest Research Ltd., HTW-016, fgr.nz/documents/download/3763, 2015.

[12] Leitner S., et al.,Technical, Safety and Environmental Challenges in the Electrification of Cable Yarding Equipment. *Current Forestry Reports*, Vol.9, pp.263-275, 2023.

[13] Leitner S., Vidoni R., Performance and Efficiency Study of a Hybrid Self-Propelled Cable Logging Carriage – Preliminary Results. *Advances in Italian Mechanism Science*, pp.171-182, 2024.

[14] Cadei A., et al.,Energy Efficiency of a Hybrid Cable Yarding System: A Case Study in the North-Eastern Italian Alps under Real Working Conditions. *Journal of Agricultural Engineering*, 52, no. 3, 2021.

[15] Leitner S., Renzi M., Spinelli R., Vidoni R., On the Design of Hybrid Tower Yarder Drivetrains: A Case Study. *Forests*, 13, 1520, 2022.

[16] Leitner S., et al., Requirements and Challenges in the Design and Potential of Smart and Efficient Winch Assisted Forestry Machinery. *Lecture Notes in Civil Engineering*, vol 337. Springer, Cham., 2022.

[17] Leitalpin GmbH.; Projects. September 2024, [Online]. Available: http://www.leitalpin.com/en

[18] IOR energy, “Engineering Conversion Factors”, https://web.archive.org/web/20100825042309/... http://www.ior.com.au/ecflist.html, accessed 01.04.2024